

Elsevier Editorial System(tm) for The International Journal of Biochemistry & Cell
Biology
Manuscript Draft

Manuscript Number: BC-D-15-00036R1

Title: Osteogenic differentiation of human MSCs: specific occupancy of the mitochondrial DNA by NFATc1 transcription factor.

Article Type: Short Communication

Keywords: osteogenic differentiation; mesenchymal stem cells; mitochondria; NFATc1; chromatin immunoprecipitation assay.

Corresponding Author: Prof. Roberta Piva, Ph.D.

Corresponding Author's Institution: University of Ferrara

First Author: Elisabetta Lambertini

Order of Authors: Elisabetta Lambertini; Letizia Penolazzi; Claudia Morganti; Gina Lisignoli; Nicoletta Zini; Marco Angelozzi; Massimo Bonora; Letizia Ferroni; Paolo Pinton; Barbara Zavan; Roberta Piva, Ph.D.

Manuscript Region of Origin: ITALY

Dear Editor,

enclosed please find the revised version of our manuscript (BC-D-15-00036) entitled: “*Osteogenic differentiation of human MSCs: specific occupancy of the mitochondrial DNA by NFATc1 transcription factor.*” by Elisabetta Lambertini, Letizia Penolazzi, Claudia Morganti, Gina Lisignoli, Nicoletta Zini, Marco Angelozzi, Massimo Bonora, Paolo Pinton, Barbara Zavan and myself.

As required, we revised our manuscript addressing the comments of the referees. A detailed response to the concerns of the reviewers has been attached. In addition, we have also considered the editorial points:

1. the manuscript has been revised for the English language
2. the Abstract has been completely revised taking into account editorial comments

Looking forward for your comments, we thank you in advance for your kind consideration.

Sincerely yours,

Prof. Roberta Piva

Dipartimento di Scienze Biomediche e Chirurgico Specialistiche,
Università di Ferrara,
Via Fossato di Mortara, 74
44121 FERRARA – Italy

phone (39)-532-974405

E-mail address: piv@unife.it

Response to reviewers' comments:

Reviewer #1: thank you very much for your positive comments.

In our brief report the involvement of NFATc1 as a negative regulator of mitochondrial function has been reported for the first time. In order to better explain our hypothesis, we improved the last part of the discussion.

Reviewer #2:

Thank you for your comments. I would like to clarify the following:

Understanding the complexity of mesenchymal stem cell (MSC) differentiation requires methods that are able to capture also slight changes in the dynamics of the process, such as those regarding the localization and unexpected DNA binding of a transcriptional regulator.

In this perspective, identifying the recruitment of NFATc1 at the regulatory region of mtDNA only when osteo-induced MSC effectively reach the maximum level of differentiation is the demonstration of a positive correlation between this transcription factor (which may exert its role only when is recruited at chromatin level) and a precise phenomenon (deposition of mineral matrix). Certainly, our evidence has to be studied in more detail, in particular to understand the relationship with the process of final differentiation, quiescence, senescence and apoptosis. Our data are the basis for investigating novel molecular regulatory circuits correlated with energetic metabolism by using appropriate experimental models, and we are working in this direction.

In the case of osteogenesis the achievement of the final differentiation state leads to mature/quiescent osteocytes from committed osteoblasts buried inside the bone matrix, and remaining osteoblasts which finish their mineralization process and die by apoptosis.

During in vitro osteogenic differentiation, we refer mainly to the activities and functions of progenitor cells that become osteoblasts. Conventional in vitro conditions for hMSC osteogenic differentiation, show that about 28 days of culture are needed to produce a layer of cells mainly represented by osteoblasts that are passively embedded into the mineralized matrix that they themselves produced. Beyond this period the functionality of cell aggregate in culture is impaired since the cells undergo senescence and apoptosis as well as occurs in vivo. Accordingly, the activity of mitochondria in this artificial bone stem cell niche supporting osteogenic differentiation, changes dramatically. As we shortly discussed in the paper, the high energy aerobic demand by osteoblasts characterizing the early stages of differentiation, is then necessarily slowed down during the progress of calcified matrix deposition and at the end of differentiation when the cells become apoptotic or quiescent. The regulation of these dynamics is still poorly studied even if it is reasonable that specific signals are sent from the nucleus to mitochondria to change their activities. Our data seem to support this hypothesis, suggesting that one of these signals can be represented by NFATc1 transcription factor that appears to have a negative role in the control of transcription of mitochondrial DNA. These evidences are in agreement with the role of NFATc1 in the calcification process and osteogenic differentiation. It may be reasonable assumed that in the nucleus NFATc1 acts as a positive factor promoting the expression of proteins required for the terminal differentiation, including the components of the extracellular matrix, while in the mitochondrion can act as a negative factor by interrupting the aerobic energy demand that is no longer needed. In order to clarify our hypothesis, we improved the last part of the discussion.

Specific minor comments:

Abstract, line 6: the studies described in the manuscript are 'in vitro', not 'in vivo'.

The term "in vivo" refers only to Chromatin Immunoprecipitation (ChIP) experiments.

ChIP is a powerful technique for examining transcription factor recruitment to chromatin, at the level of specific genomic sequences. This technique is based on covalent cross-linking of DNA and proteins with formaldehyde treatment performed on freshly cultured cells and, for this reason, the analysis leads to the identification of an “in vivo” interaction.

Careful editing by a native English speaker who understands the scientific content is required, e.g. p. 3, para. 1, line 13: 'informations' should be 'information'. There are many more examples of incorrect English expression.

The manuscript has been entirely revised for the English language.

p. 4, section 2.1: there needs to be a brief description of the source, isolation and characterization of hMSCs, rather than just referring to a paper.

We added the required information in the Materials and methods section. Moreover, immunophenotypic characterization using flow cytometry have been added as supplemental data (see new version of Supplemental Fig.1).

p. 5, para. 1: there is no explanation of how mRNA levels were calculated from the quantitative PCR data. They are described as 'mRNA relative quantification' in the figure, but it is unclear what the values are relative to.

The required information has been added in the Materials and methods section and Fig.1 legend has been implemented.

p. 5, sections 2.3 and 2.4: there is inadequate description of the immunocytochemical methods. For the primary antibodies the species of the immunogen and the species the antibody is made in should be included. The detection antibodies also need to be described. It is not enough to say 'Cells were then incubated in Vecstain ABC', or 'primary antibodies were revealed by means of appropriate AlexaFluor 488 conjugated'. The latter is not a complete sentence.

The description of Immunocytochemistry and Immunofluorescence has been improved.

p. 7, line 7: is 'semiquantitative PCR' the correct term?

Yes, the term “semiquantitative PCR” is correct. In semi-quantitative conventional PCR the input DNA positive control is utilized to demonstrate the equal amount of chromatin in the different experiments.

p. 7, section 3.1: This section should be in the Methods section (see comment above about description of hMSCs).

Section 3.1 has been removed and moved to the 2.1 Materials and methods section.

Figure 2C: This EM image is not particularly convincing. It should be presented in parallel with a lower power image including part of a nuclear profile.

Additional experiments have been performed and a new image including part of a nuclear profile has been added (see new version of Fig. 2C).

The figure legends are too long. Any information that duplicates information in the Methods section should be removed from the legend. Any detail on methods that is not duplicated should be moved to the Methods section.

All Figure legends have been shortened and some details have been moved to the Materials and methods section.

Osteogenic differentiation of human MSCs: specific occupancy of the mitochondrial DNA by NFATc1 transcription factor.

Elisabetta Lambertini^a, Letizia Penolazzi^a, Claudia Morganti^b, Gina Lisignoli^c, Nicoletta Zini^{d,e}, Marco Angelozzi^a, Massimo Bonora^b, Letizia Ferroni^f, Paolo Pinton^b, Barbara Zavan^f, Roberta Piva^{a*}

^a *Department of Biomedical and Specialty Surgical Sciences, University of Ferrara, Ferrara, Italy*

^b *Section of Pathology Oncology, Experimental Biology Laboratory for Technologies of Advanced Therapies (LTTA), Department of Morphology, Surgery, Experimental Medicine University of Ferrara, Ferrara, Italy*

^c *Laboratorio di Immunoreumatologia e Rigenerazione Tissutale, IOR, Bologna, Italy*

^d *CNR – National Research Council of Italy, Institute of Molecular Genetics, Bologna, Italy*

^e *Laboratory of Musculoskeletal Cell Biology, Istituto Ortopedico Rizzoli, Bologna, Italy*

^f *Department of Biomedical Sciences, University of Padova, Padova, Italy*

* Corresponding author at: Department of Biomedical and Specialty Surgical Sciences, University of Ferrara, Via Fossato di Mortara, 74 44121, Ferrara, Italy.

Tel.: +39 0532974405; fax: +39 0532974405.

E-mail address: piv@unife.it

ABSTRACT

Several evidences indicate that mitochondrial morphology and function change during osteogenic differentiation. However, molecular mechanisms linking mitochondrial dynamics with the regulation of osteoblast functions are poorly understood. Among the molecules that influence the decision of human mesenchymal stem cells (hMSCs) to become osteoblasts are Slug and NFATc1 transcription factors (TFs). These molecules also interfere with different mitochondria-dependent pathways in response to a variety of cellular demands. In the present study we investigated the recruitment of Slug and NFATc1 at the D-loop regulatory region of mitochondrial DNA (mtDNA) in osteogenic differentiated hMSCs. Our aim is to explore whether Slug and NFATc1 can also act as mitoTFs in the mitochondrial pool of nuclear TFs.

For the first time, we demonstrated that NFATc1, but not Slug, is localized in the mitochondria. Using chromatin immunoprecipitation assay, we found that NFATc1 is “in vivo” recruited at mtDNA. This occurs only when the calcification process is at its highest in osteo-induced MSC and the maximum level of differentiation is reached. Furthermore, the occupancy of the mtDNA by NFATc1 is associated with a decreased expression of crucial mitochondrial genes such as Cytochrome B and NADH dehydrogenase 1. This suggests that NFATc1 acts as negative regulator of mtDNA transcription during the calcification process and interruption of aerobic energy demand. Therefore, the finding of NFATc1 participation in osteogenic differentiation through its direct involvement in the regulatory machinery of mitochondria suggests a new role for this TF and add information on communication between mitochondrial and nuclear genomes.

Keywords:

osteogenic differentiation

mesenchymal stem cells

mitochondria

NFATc1

chromatin immunoprecipitation assay

1. Introduction

It is well known that variations of number, structure, function and intracellular distribution of mitochondria are correlated with cell functionality and different cell energy demand (Kuznetsov and Margreiter, 2009). These variations, which are strictly associated with a finely tuned crosstalk between the mitochondrial and nuclear genomes, have only been recently appreciated as essential events during the differentiation process of stem cells and cell fate switch (Parker et al., 2009; Mandal et al., 2011; Folmes et al., 2012; Bukowiecki et al., 2014; Wanet et al., 2014). While numerous efforts have been made to uncover the mechanisms of mitochondrial biogenesis as well as to characterize energy metabolism and redox status during cell differentiation (Chen et al., 2008; Chen et al., 2010; Madeira, 2012), little is known about mitochondria transcription regulation by lineage-specific factors and signaling demands. In particular, molecular regulatory circuits that govern mitochondrial dynamics together with mitochondrial contribution to differentiation potential of stem cells remain poorly understood. Thus it is important to explore the properties of mitochondria during differentiation of cellular progenitors. This may add new information on stem cell biology, and may help developing new pharmacologic strategies in regenerative medicine. In addition, this may facilitate the understanding of maintenance of cell culture homeostasis and the optimization of *in vitro* cell differentiation protocols by adjusting some biochemical properties, such as energy production or redox status of mitochondria. These improvements may provide high quality stem cells to be used for cell therapy. In this scenario, mitochondrial properties might thus be used as a quality measure of cell-based products for several clinical use.

Recent studies showed that mitochondrial DNA copy number, protein subunits of the respiratory enzymes, and intracellular ATP content, increased together with the efficiency of oxidative phosphorylation during osteogenic differentiation of adult human mesenchymal stem cells (hMSCs) (Chen et al., 2008; Pietilä et al., 2010). Growing evidence supports the bifunctional role of many transcription factors (TFs) in the control of both nuclear and mitochondrial gene expression (Szczepanek et al., 2012; Leigh-Brown et al., 2010).

Two nuclear TFs, Slug/Snail2 (Cobaleda et al., 2007) and NFATc1 (nuclear factor of activated T cells complex 1) (Horsley and Pavlath, 2002), have been recently described as osteogenic modulators (Lambertini et al., 2009; Deng et al., 2008; Koga et al., 2005; Penolazzi et al., 2011).

Slug belongs to the highly conserved Slug/Snail family of transcription factors with an essential role in development and in many cellular functions including control of stem cell properties (Cobaleda et al., 2007). NFAT proteins comprise a family of transcription factors (NFAT 1-5) that,

after calcium/calcineurin-dependent dephosphorylation, are activated and regulate the expression of many genes involved in a wide range of cellular processes (Hogan et al., 2003).

Up to now it is unexplored if Slug and NFATc1 are possible mitoTFs in the mitochondrial pool of nuclear TFs. Several evidences indicate that these TFs are associated with mitochondria functions. In particular, Slug interferes with the mitochondria-dependent apoptotic pathway (Wu et al., 2005), may regulate mitochondrial ROS production (Kim et al., 2011), and supports the propagation of stress signaling transcriptional network organized by CREB and HMGA2 in mitochondrial dysfunction (Shibanuma et al., 2012). NFATc1, through calcineurin and calmodulin, is implicated in the regulation of gene expression by calcium signaling, the control of which involves the mitochondria (Kim et al., 2009; Chen et al., 2007; Stern, 2006).

Starting from these evidences, we aimed to further characterize mitochondria during differentiation of hMSCs towards osteogenesis, and examine whether osteogenic transcription factors (TFs) are also present in the mitochondria. Furthermore, we studied whether Slug and NFATc1 can be good candidates in the communication between mitochondrial and nuclear genomes, and can contribute to the behavior of MSCs in differentiating towards osteogenic lineage through the regulation of mitochondrial gene expression.

2. Materials and methods

2.1 Cell Culture and differentiation

Human mesenchymal stem cells (hMSC) were isolated from human adipose tissues of five healthy women and 5 healthy men (age: 21-36) undergoing cosmetic surgery procedures at the University of Padova's Plastic Surgery Clinic. The adipose tissues were digested with 0.075% collagenase (type 1A; Sigma-Aldrich Chemical Co., St. Louis, MO) in a modified Krebs-Ringer buffer (KRB) [125 mM NaCl, 5mM KCl, 1mM Na₃PO₄, 1mM MgSO₄, 5.5 mM glucose, and 20mM Hepes (pH 7.4)] for 60' at 37°C, followed by 10' with 0.25% trypsin. Floating adipocytes were discarded, and cells from the stromal-vascular fraction were pelleted, rinsed with media, and centrifuged (Gardin et al., 2011). The resulting viable cells were counted using the trypan blue exclusion assay and seeded at a density of 10⁶ cells per cm² for *in vitro* expansion, in Dulbecco's modified Eagle's medium low-glucose supplemented with 10% fetal bovine serum (Euroclone S.p.A., Milan, Italy), 2mM L-glutamine, antibiotics (penicillin 100 µg/mL and streptomycin 10 µg/mL), at 37 °C in a humidified atmosphere of 5% CO₂.

hMSCs were used at passage 3 and characterized by testing a panel of surface markers using flow cytometry as previously described (Torreggiani et al., 2012). hMSC from all samples were positive for CD90, CD73, CD105 (mesenchymal cell markers), but negative for CD34, and CD45 (haematopoietic cell markers) (Supplemental Fig.1A). Multilineage differentiation potentials in response to specific differentiating agents have been confirmed in all samples analyzed. As reported in Supplemental Fig. 1B, Alizarin Red staining revealed the ability of the cells to deposit mineral matrix that is a characteristic of osteoblastic lineage, Alcian Blue stains sulfated proteoglycans deposits that are indicative of chondrogenic differentiation, and Oil Red-O staining demonstrated the formation of lipid droplets after induction of adipogenic differentiation.

For osteogenic differentiation, hMSCs were cultured up to 28 days in DMEM High Glucose (Euroclone S.p.A.) supplemented with 10% FBS, 10mM β -glycerophosphate, 10^{-7} M dexamethasone and 100 mM ascorbate (Sigma-Aldrich). For Alizarin Red S (ARS) staining, the cells were fixed with 70% ethanol for 1 hour and then stained with 40 mM Alizarin Red S solution (pH 4.2) at room temperature for 10'. Cells were microphotographed by an optical Leitz microscope.

2.2 Quantitative Real-Time RT-PCR

Cells were harvested and total RNA was extracted using an RNeasy Mini Kit (Qiagen, Hilden, Germany) in accordance with the manufacturer's instruction. Quantitative real-time PCR was performed using gene expression Master mix (Life Technologies, Carlsbad, CA, USA) and analyzed on CFX96 Real-Time detection System (Bio-Rad laboratories, Hercules, CA, USA). Assays-On-Demand kits (Life Technologies) for human *OC*, *ON*, *OPN*, *Runx2*, *COL1A1*, *ALP*, *BMP2*, *BMP7*, *Slug*, *NFATc1*, *ND1* and *CYTB* were used. For the PCR analysis, target gene expression levels were normalized using GAPDH endogenous control and relative mRNA levels were calculated using the $2^{-\Delta\Delta CT}$ method. All data are expressed as the mean of Technical triplicates of six hMSCs samples.

2.3 Immunocytochemistry

hMSC grown in chamber slides were fixed in ice-cold methanol and then permeabilized with 0.2% (v/v) Triton X-100 (Sigma-Aldrich) in TBS (Tris-buffered saline). After blocking with 2% normal horse serum (Vectorlabs, Burlingame, CA, USA), hMSCs were incubated with primary antibody for 16 hours at 4°C. The following primary antibodies were used: rabbit anti-human Col1A1 (H-

197, 1:100), rabbit anti-human OPN (LF-123, 1:100) and rabbit anti-human RUNX2 (M-70, 1:100) (Santa Cruz Biotechnology, Dallas, TX, USA). Cells were then rinsed and incubated with ImmPRESS™ (Peroxidase) Polymer Universal Anti-Mouse/Rabbit Ig Reagent (Vectorlabs) for 30'. After washing, the cells were stained with Vectastain ABC reagent and DAB substrate kit for peroxidase (Vectorlabs), mounted in glycerol/TBS 9:1 and observed using a Leitz microscope.

2.4 Immunofluorescence and confocal analysis

hMSC were stained with 100 nM Mitotracker Orange CMTMRos (Life Technologies) for 15' at 37°C and fixed in 4% paraformaldehyde/PBS. After three washes with TBS, the cells were permeabilized with 0.2% Triton X-100 and then blocked with TBS 2.5% FCS. Cells were then incubated over night at 4°C with antibodies (Santa Cruz) against human NFATc1 (clone H-110, 1:20), SLUG (clone H-140, 1:20), TFAM (clone H-203, 1:100). Finally primary antibodies were revealed by means of Alexa Fluor® 488 Goat Anti-Rabbit IgG (H+L) (1:100) (Life Technologies). Images were acquired on Axiovert 220M microscope equipped with a x100 oil immersion Plan-Neofluar objective (NA 1.3, from Carl Zeiss, Jena, Germany) and a CoolSnap HQ CCD camera. The acquired images were background corrected, and Pearson's coefficient for co-localization was analyzed using JACOP plugin of the open source Fiji software (<http://fiji.sc/Fiji>).

2.5 Immunogold labeling and electron microscopy

hMSCs were fixed in 1% glutaraldehyde in 0.1M phosphate buffer pH7.4 for 1 hour, partially dehydrated up to 70% ethanol and embedded in London Resin White (LR White) at 0°C. Thin sections were pre-incubated with 5% normal goat serum in 0.05M Tris-Cl, pH 7.6, 0.14M NaCl, 0.1% BSA (TBS I) and then incubated overnight at 4°C with rabbit anti-human NFATc1 (Santa Cruz, clone H-110, 1:10 dilution in TBS I); and then with a goat anti-rabbit conjugated with 15-nm colloidal gold particles (BBInternational, Cardiff, UK) diluted 1:20 in 0.02M Tris-HCl, pH 8.2, 0.14M NaCl and 0.1% BSA for 1 hour at room temperature. Thin sections were stained with aqueous uranyl acetate and lead citrate and observed with a Zeiss EM109 transmission electron microscope. Images were captured using a Nikon digital camera Dmx 1200F, and ACT-1 software.

2.6 Subcellular fractionation and western blot analysis

hMSCs were harvested and gently disrupted by homogenization as reported (Bononi and Pinton, in press). The homogenate was centrifuged twice at 1000 g for 5' to remove nuclei and unbroken cells (nuclear fraction) and then the supernatant was centrifuged 10000 g for 10'. The resultant supernatant was used for cytosolic fraction isolation, while the pellet, consisting in the mitochondrial fraction, was subjected to 100 μ M Proteinase K (Sigma-Aldrich) for 30' on ice. Proteins from the three subcellular fractions were electrophoresed on 12% SDS-polyacrylamide gel and transferred onto an Immobilon-P PVDF (Millipore, Billerica, MA). After blocking the following primary antibodies were used: VDAC (mouse anti-human, 1:2000, Millipore, Billerica, MA), Lamin B1 (mouse anti-human, 1:1000, Santa Cruz) and NFATc1 (rabbit anti-human, 1:500, Santa Cruz Biotechnology). After washing, the membranes were incubated with HRP-conjugated anti-mouse (1:2000) or anti-rabbit (1:50000) antibodies (Dako, Glostrup, Denmark) and signals were detected by SupersignalWest Femto Substrate (Pierce, Rockford, IL, USA).

2.7 Chromatin Immunoprecipitation (ChIP)

ChIP assay was done using a ChIP Assay Kit (catalog no. 17-295) from Upstate following procedures provided by the manufacturer. Briefly, after crosslinking the chromatin with 1% formaldehyde at 37°C for 10', cells were washed with cold PBS, scraped and collected on ice, lysed and sonicated. An equal amount of chromatin was immunoprecipitated at 4°C overnight with 5 μ g of the following antibodies: TFAM, Slug, NFATc1, or non-specific IgG (Santa Cruz). Immunoprecipitated products were collected after incubation with Protein A-agarose beads. The beads were washed, and the bound chromatin was eluted in ChIP Elution Buffer. The samples were incubated at 65°C overnight to reverse the crosslinking. Then the proteins were digested with Proteinase K for 1 h at 45°C and DNA was purified in 50 μ L of Tris-EDTA with a PCR purification kit (Qiagen) according to the manufacturer's instructions. The DNA precipitates and Input (1% of total chromatin used for the immunoprecipitation) were further subjected to semi-quantitative or quantitative PCR using the following primers for amplification of 286-bp fragment of the D-loop region (d-loop forward, 5'-CCC CTC ACC CACTAGGATAC-3', and d-loop, reverse, 5'-ACG TGT GGG CTA TTT AGG C-3'). PCR products were analyzed by agarose gel electrophoresis and visualized by UV light apparatus. Real-time PCR analyses of the ChIP samples were carried with CFX96 Real-Time detection System (Bio-Rad labs) using iTaq Universal SYBR Green SuperMix (Bio-Rad). We analyzed ChIP-qPCR data relative to Input signal and presented as fold increase in signal relative to the background signal (IgG).

2.8 Statistical analysis

The Student's t test was used for comparisons between the groups. $P < 0.05$ was considered significant.

3. Results and discussion

3.1. hMSC osteogenic differentiation and mitochondria

We focused on the ability of hMSCs to differentiate towards osteoblastic lineage in order to add informations on functional link between mitochondria and osteogenic differentiation. As shown in Fig. 1A and B, osteogenic induced cells increased the expression of typical osteogenic markers. These include: the main constituent of the organic part of the bone extracellular matrix (ECM) Collagen type I (Col1A1), alkaline phosphatase (ALP) which is responsible for the ECM mineralization, the master regulator of osteogenic differentiation runt-related transcription factor 2 (Runx2), three non-collagenous ECM proteins, osteopontin, osteonectin and osteocalcin, three osteogenic growth factors (BMP2, BMP7 and WNT3). Moreover, the cells produced Alizarin red positive nodular aggregates at the end of differentiation (day 28).

The mitochondrial morphology has been then assessed by Mitotracker Orange staining at early stage of osteogenic differentiation (day 14) when oxidative demand induced by osteogenic medium is high. As shown in Fig. 1C, relative mitochondrial network area per cell was significantly increased in osteogenic induced cells, while no significant alterations were observed in average particle area or form factor.

There are many open questions regarding the signaling pathways and key molecules supporting mitochondria changes in response to specific cell processes such as osteogenic differentiation. The need to respond to this issue is important both for defining the complexity of human mitochondrial transcription machinery, and for understanding the increasing number of diseases associated with mitochondrial dysfunction. Specifically, this approach may be useful to provide new information toward the development of novel therapeutics for bone disorders and bone tissue regeneration.

3.2. NFATc1, but not Slug, is associated with mitochondria

By qRT-PCR analysis we confirmed that hMSCs express substantial levels of Slug and NFATc1 transcription factors both at basal condition (day 0) and after osteogenic differentiation. In

particular, mRNA for Slug significantly increased in osteogenic differentiated hMSCs compared to undifferentiated ones (Fig. 2A).

In-silico analysis allows prediction of NFATc1 and Slug localization to mitochondria. Such predictions were performed by two different informatical tools, MitoProt and TargetP. Both these tools predict high probability for mitochondrial localization of some NFATc1 isoforms, while only MitoProt predicts a slight probability for Slug to reach mitochondria (Table 1).

NFATc1 and Slug localization were then investigated by immunostaining and confocal microscopy co-localization analysis (Fig. 2B). Interestingly, NFATc1 displays significant co-localization with the mitochondrial marker Mitotracker Orange (as indicated by Pearson's coefficient) to an extent comparable to the Transcription factor A mitochondrial (TFAM) which is a crucial activator of mitochondrial transcription and genome duplication. On the contrary, Slug remains predominantly localized to the nucleus. Immunogold labeling and Western blot analysis confirmed the association of NFATc1 with the mitochondria (Fig. 2C, D).

Treatment with osteogenic inducers did not affect the localization of these two bone associated transcription factors (data not shown).

3.3. NFATc1 is recruited at mtDNA

In order to explore functional regulatory role of Slug and NFATc1 nuclear transcription factors in mitochondria, we performed a chromatin immunoprecipitation (ChIP) assay to analyze the "in vivo" recruitment of Slug and NFATc1 at the non-coding displacement loop (D-loop) regulatory region of mtDNA (Hock and Kralli, 2009). It is well known that mitochondrial genes are densely packed along the genome with the exception of D-loop which is devoted to transcription initiation carried out by the mitochondrial-specific RNA polymerase (Shutt et al., 2011; Marinov et al., 2014).

Multiple reports have suggested that TFs, that typically act in the nucleus, might also have regulatory functions in mitochondrial transcription (Leigh-Brown et al., 2010; Hock and Kralli, 2009; Szczepanek et al., 2012). These include: CREB, NF-kB, ER, MEF2D, STAT1, T3 receptor p43, p53, IRF3, and STAT3. However, a direct evidence of in vivo protein-DNA contacts in mitochondria has been provided by ChIP analysis only for p53, CREB, and MEF2D (Leigh-Brown et al., 2010).

By using the programs Transcription Element Search Software (TESS) for TF search, and MatInspector 7.4, we identified the presence of one putative Slug binding site (E-box motifs, 5'-CACCTG/CAGGTG-3') and three NFAT binding sites (5'-GGAAA-3') in the D-loop region (Fig. 3A).

The results from ChIP assays demonstrated that in all examined conditions Slug is not recruited at appreciable levels. Interestingly, in hMSC samples that fail osteogenic differentiation the D-loop region chromatin was not immunoprecipitated by neither Slug nor by NFATc1 (see the n.2 representative sample in Fig. 3A). Conversely, the D-loop region is highly occupied by NFATc1 in hMSCs that undergo osteogenesis and this recruitment increased when the cells reach the end of the differentiation process (day 28). TFAM, which is required for initiation and regulation of mitochondrial transcription, was properly recruited by its recognition site at a very high level regardless of the presence of differentiating agents. Recent studies demonstrated that mitochondria are maintained at a low activity state in hMSCs. Upon osteogenic induction, their functions increased to fulfill a higher degree of energy demand or to facilitate other biochemical reactions that take place within the organelles. However, the high energy aerobic demand by osteoblasts at the early stages of differentiation, is necessarily slowed down during the progress of calcified matrix deposition and, even more, at the end of differentiation when the cells become apoptotic or quiescent. The regulation of these dynamics is still poorly studied even if it is reasonable that specific signals are sent from the nucleus to mitochondria to change their activities (Cagin and , 2015). Our data are consistent with this hypothesis, suggesting that one of these signals could be represented by NFATc1 acting as negative regulator of mtDNA transcription. Therefore, NFATc1 could contribute to the calcification process participating in the interruption of aerobic energy demand when is no longer needed (see the scheme in Fig. 3B).

This hypothesis is furthered by the expression levels of crucial mitochondrial genes. As shown in Fig. 3C, we observed a decrease of CytB (Cytochrome B) and ND1 (NADH dehydrogenase 1) expression at the end of the osteogenic differentiation.

Concerning NFATc1 in osteoblasts, our preliminary evidences can shed light on the controversial role of NFATc1 in osteoblastic differentiation and function. Recent studies have demonstrated that activation of NFATc1 promotes osteoblast differentiation *in vitro* and *in vivo* (Koga et al., 2005; Fromigue et al., 2010, Ogasawara et al., 2013). Other evidences support the inhibitory effects of NFATc1 on osteoblast differentiation through different pathways (Yeo et al., 2007; Zanotti et al., 2011). Therefore, the role of NFATc1 in osteoblasts could be different, depending on its interaction with other specific molecules.

In addition, concerning the potential involvement of NFATc1 in mineralization process, our data are in agreement with recent evidences that indicate the implication of this transcription factor in vascular calcification (Goettsch et al., 2011).

In conclusion, our data suggest a new role of NFATc1, even if further studies are required for a better understanding of its involvement in the regulatory machinery of mitochondria in relation to osteoblast function and energetic metabolism.

Conflict of interest statement

No conflicts of interest, financial or otherwise, are declared by the authors.

Acknowledgements

This work was supported by Fondazione Cassa di Risparmio di Padova e Rovigo, Italy.

References

Bononi A, Pinton P. Study of PTEN subcellular localization. *Methods*, in press.

Bukowiecki R, Adjaye J, Prigione A. Mitochondrial function in pluripotent stem cells and cellular reprogramming. *Gerontology* 2014;60:174-182.

Cagin U, Enriquez JA. The complex crosstalk between mitochondria and the nucleus: What goes in between? *Int J Biochem Cell Biol*, in press.

Chen CT, Hsu SH, Wei YH. Upregulation of mitochondrial function and antioxidant defense in the differentiation of stem cells. *Biochim Biophys Acta* 2010;1800:257-263.

Chen CT, Shih YR, Kuo TK, Lee OK, Wei YH. Coordinated changes of mitochondrial biogenesis and antioxidant enzymes during osteogenic differentiation of human mesenchymal stem cells. *Stem Cells* 2008;26:960-968.

Chen Y, Yuen WH, Fu J, Huang G, Melendez AJ, Ibrahim FB, Lu H, Cao X. The mitochondrial respiratory chain controls intracellular calcium signaling and NFAT activity essential for heart formation in *Xenopus laevis*. *Mol Cell Biol* 2007;27:6420-6432.

Cobaleda C, Pérez-Caro M, Vicente-Dueñas C, Sánchez-García I. Function of the zinc-finger transcription factor SNAI2 in cancer and development. *Annu Rev Genet* 2007;41:41-61.

Deng ZL, Sharff KA, Tang N, Song WX, Luo J, Luo X, Chen J, Bennett E, Reid R, Manning D, Xue A, Montag AG, Luu HH, Haydon RC, He TC. Regulation of osteogenic differentiation during skeletal development. *Front Biosci* 2008;13:2001-2021.

Folmes CD, Dzeja PP, Nelson TJ, Terzic A. Mitochondria in control of cell fate. *Circ Res* 2012;110:526-529.

Fromigue O, Hay E, Barbara A, Marie PJ. Essential role of nuclear factor of activated T cells (NFAT)-mediated Wnt signaling in osteoblast differentiation induced by strontium ranelate. *J Biol Chem* 2010;285:25251-25258.

Gardin C, Vindigni V, Bressan E, Ferroni L, Nalesso E, Puppa AD, D'Avella D, Lops D, Pinton P, Zavan B. Hyaluronan and fibrin biomaterial as scaffolds for neuronal differentiation of adult stem cells derived from adipose tissue and skin. *Int J Mol Sci* 2011;12:6749-6764.

Goettsch C, Rauner M, Hamann C, Sinnigen K, Hempel U, Bornstein SR, Hofbauer LC. Nuclear factor of activated T cells mediates oxidised LDL-induced calcification of vascular smooth muscle cells. *Diabetologia* 2011;54:2690-2701.

Hock MB, Kralli A. Transcriptional control of mitochondrial biogenesis and function. *Annu Rev Physiol* 2009;71:177-203.

Hogan PG, Chen L, Nardone J and Rao A. Transcriptional regulation by calcium, calcineurin, and NFAT. *Genes Dev* 2003;17:2205-2232.

Horsley V, Pavlath GK. NFAT: ubiquitous regulator of cell differentiation and adaptation. *J Cell Biol* 2002;156:771-774.

Kim CH, Jeon HM, Lee SY, Ju MK, Moon JY, Park HG, Yoo MA, Choi BT, Yook JI, Lim SC, Han SI, Kang HS. Implication of snail in metabolic stress-induced necrosis. *PLoS One* 2011;6:e18000.

Kim MS, Usachev YM. Mitochondrial Ca²⁺ cycling facilitates activation of the transcription factor NFAT in sensory neurons. *J Neurosci* 2009;29:12101-12114.

Koga T, Matsui Y, Asagiri M, Kodama T, de Crombrughe B, Nakashima K and Takayanagi H. NFAT and Osterix cooperatively regulate bone formation. *Nat Med* 2005;11:880-885.

Kuznetsov AV, Margreiter R. Heterogeneity of mitochondria and mitochondrial function within cells as another level of mitochondrial complexity. *Int J Mol Sci* 2009;10:1911-1929.

Lambertini E, Lisignoli G, Torreggiani E, Manferdini C, Gabusi E, Franceschetti T, Penolazzi L, Gambari R, Facchini A, Piva R. Slug gene expression supports human osteoblast maturation. *Cell Mol Life Sci* 2009;66:3641-3653.

Leigh-Brown S, Enriquez JA, Odom DT. Nuclear transcription factors in mammalian mitochondria. *Genome Biol* 2010;11:215.

Madeira VM. Overview of mitochondrial bioenergetics. *Methods Mol Biol* 2012;810:1-6.

Mandal S, Lindgren AG, Srivastava AS, Clark AT, Banerjee U. Mitochondrial function controls proliferation and early differentiation potential of embryonic stem cells. *Stem Cells* 2011;29:486-495.

Marinov GK, Wang YE, Chan D, Wold BJ. Evidence for site-specific occupancy of the mitochondrial genome by nuclear transcription factors. *PLoS One* 2014;9:e84713.

Ogasawara T, Ohba S, Yano F, Kawaguchi H, Chung UI, Saito T, Yonehara Y, Nakatsuka T, Mori Y, Takato T, Hoshi K. Nanog promotes osteogenic differentiation of the mouse mesenchymal cell line C3H10T1/2 by modulating bone morphogenetic protein (BMP) signaling. *J Cell Physiol* 2013;228:163-171.

Parker GC, Acsadi G, Brenner CA. Mitochondria: determinants of stem cell fate? *Stem Cells Dev* 2009; 18: 803-806.

Penolazzi L, Lisignoli G, Lambertini E, Torreggiani E, Manferdini C, Lolli A, Vecchiatini R, Ciardo F, Gabusi E, Facchini A, Gambari R, Piva R. Transcription factor decoy against NFATc1 in human primary osteoblasts. *Int J Mol Med* 2011;28:199-206.

Pietilä M, Lehtonen S, Närhi M, Hassinen IE, Leskelä HV, Aranko K, Nordström K, Vepsäläinen A, Lehenkari P. Mitochondrial function determines the viability and osteogenic potency of human mesenchymal stem cells. *Tissue Eng Part C Methods* 2010;16:435-445.

Shibanuma M, Ishikawa F, Kobayashi M, Katayama K, Miyoshi H, Wakamatsu M, Mori K, Nose K. Critical roles of the cAMP-responsive element-binding protein-mediated pathway in disorganized epithelial phenotypes caused by mitochondrial dysfunction. *Cancer Sci* 2012;103:1803-1810.

Shutt TE, Bestwick M, Shadel GS. The core human mitochondrial transcription initiation complex: It only takes two to tango. *Transcription* 2011;2:55-59.

Stern PH. The calcineurin-NFAT pathway and bone: intriguing new findings. *Mol Interv* 2006;6:193-196.

Szczepanek K, Lesnefsky EJ, Lerner AC. Multi-tasking: nuclear transcription factors with novel roles in the mitochondria. *Trends Cell Biol* 2012;22:429-437.

Torreggiani E, Lisignoli G, Manferdini C, Lambertini E, Penolazzi L, Vecchiatini R, Gabusi E, Chieco P, Facchini A, Gambari R, Piva R. Role of Slug transcription factor in human mesenchymal stem cells. *J Cell Mol Med* 2012;16:740-751.

Wanet A, Remacle N, Najar M, Sokal E, Arnould T, Najimi M, Renard P. Mitochondrial remodeling in hepatic differentiation and dedifferentiation. *Int J Biochem Cell Biol* 2014;54:174-185.

Wu WS, Heinrichs S, Xu D, Garrison SP, Zambetti GP, Adams JM, Look AT. Slug antagonizes p53-mediated apoptosis of hematopoietic progenitors by repressing puma. *Cell* 2005; 123:641-653.

Yeo H, Beck LH, Thompson SR, Farach-Carson MC, McDonald JM, Clemens TL, Zayzafoon M. Conditional disruption of calcineurin B1 in osteoblasts increases bone formation and reduces bone resorption. *J Biol Chem* 2007;282:35318-35327.

Zanotti S, Smerdel-Ramoya A, Canalis E. Reciprocal regulation of Notch and nuclear factor of activated T-cells (NFAT) c1 transactivation in osteoblasts. *J Biol Chem* 2011;286:4576- 4588.

Figure Legends

Fig. 1. Osteogenic differentiation of human mesenchymal stem cells (hMSCs) and evaluation of specific markers. (A) Quantitative gene expression analysis of specific osteogenic markers was performed in hMSC induced towards osteogenic differentiation for 28 days. Data analysis was performed by using the comparative threshold cycle (Ct) method and presented as variation from GAPDH expression level. Error bars represent means \pm standard deviation for n=6. *p-value <0.05 compared to Day 7 sample group. (B) Mineral matrix deposition was evaluated by ARS staining in hMSCs at day 0 and after 28 days of culture in osteogenic medium. The expression levels of Collagen type 1 (COL1A1), osteopontin (OPN) and RUNX2 were analysed by immunocytochemistry. Scale bar 50 μ m.

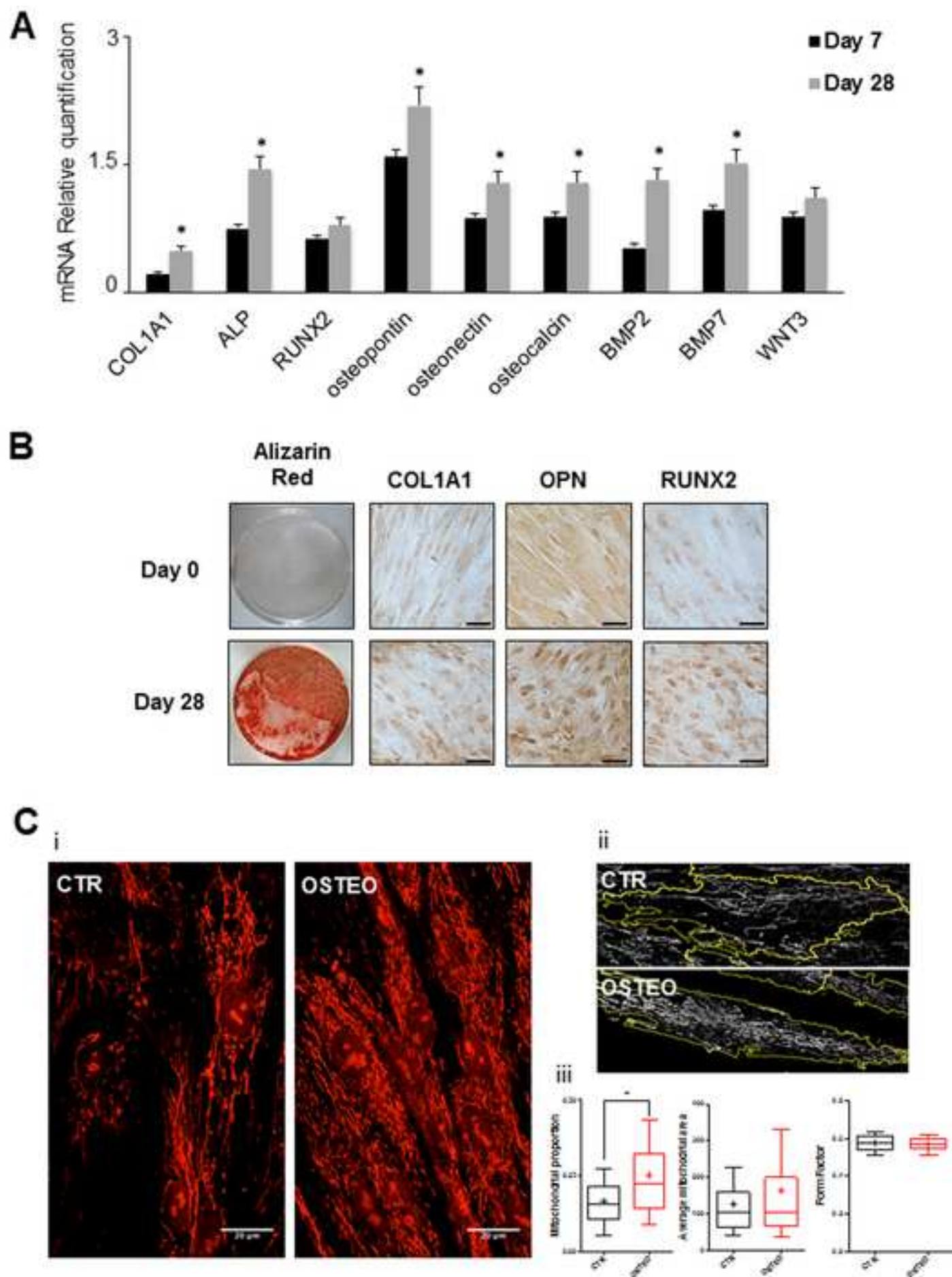
(C) Morphological aspect of hMSC mitochondria. The amount of mitochondria was evaluated by optical microscopy (i) on hMSC stained with Mitotracker Orange after 14 days of culture in presence (OSTEO) or absence (CTR) of osteogenic inducers. Images were segmented for cell surface and mitochondrial area (see representative sample in ii) to allow quantitation of relative mitochondrial amount, mitochondrial area and morphology (iii). * Significant at $p < 0.05$; line = median, cross = mean, bars = maximum and minimum values. The boxes envelop the 10th to the 90th percentile of the assayed population.

Fig. 2. Mitochondrial localization of NFATc1 and Slug. (A) Slug, and NFATc1 gene expression was determined at mRNA level in hMSCs induced towards osteogenic differentiation for 28 days, and revealed by quantitative RT-PCR. Data were normalized to GAPDH according to the formula $2^{-\Delta\Delta Ct}$ and scaled relative to day 0 expression levels. Results represent means \pm SEM of six independent experiments. *p-value <0.05 were considered statistically significant.

(B) hMSCs were treated with Mitotracker Orange (MTO, red staining) and antibodies (green staining) against TFAM, NFATc1 or Slug. Merge images represent an overlay of the two channels where co-localization is indicated by a color change (yellow). (C) Immunogold labeling of NFATc1 in mitochondria of hMSC cells. Arrows indicate gold particles; m, mitochondria; n, nucleus. (D) Nuclear (N), cytoplasmic (C) and mitochondrial (M) fractions were analyzed by Western blot for NFATc1 expression. Lamin B1 and VDAC1 were used as markers for the purity of the nuclear and mitochondrial fractions, respectively. The data are representative of three independent fractionation experiments.

Fig 3. Recruitment of Transcription factors (TFs) to the non-coding region (D-Loop) of hMSC mitochondrial DNA. (A) Schematic representation of D-Loop region with binding sites for NFAT and Slug TFs is reported. hMSCs at day 0 and after 28 days of culture in osteogenic medium were subjected to Chromatin immunoprecipitation (ChIP) assay using antibodies against Slug, NFATc1 and TFAM TFs. A non-specific IgG antibody was used as control. Representative semiquantitative PCRs after ChIP assay are shown. NTC, no template control; Input, positive control; 1, osteogenic differentiated hMSCs sample; 2, hMSCs sample unable to differentiate toward osteogenic lineage. In order to evaluate the fold enrichment relative to the IgG control, quantitative PCR was performed on osteogenic differentiated hMSCs samples. Data represent mean \pm S.E.M. (n=6). (B) The hypothesis of relationship between NFATc1 and mitochondrial activity during osteogenic differentiation of hMSCs is schematized. (C) Analysis of mt-DNA transcription in osteogenic differentiated hMSCs. Cells were cultured in presence of osteogenic inducers for 28 days and mRNA expression level of mt-CYTB and mt-ND1 was determined by quantitative RT-PCR. Data analysis was performed by using the comparative threshold cycle (Ct) method and presented as variation from GAPDH expression level. Data represent mean \pm S.E.M of six independent experiments. *p-value <0.05 compared to Day 0 sample group.

Figure 1
[Click here to download high resolution image](#)



A

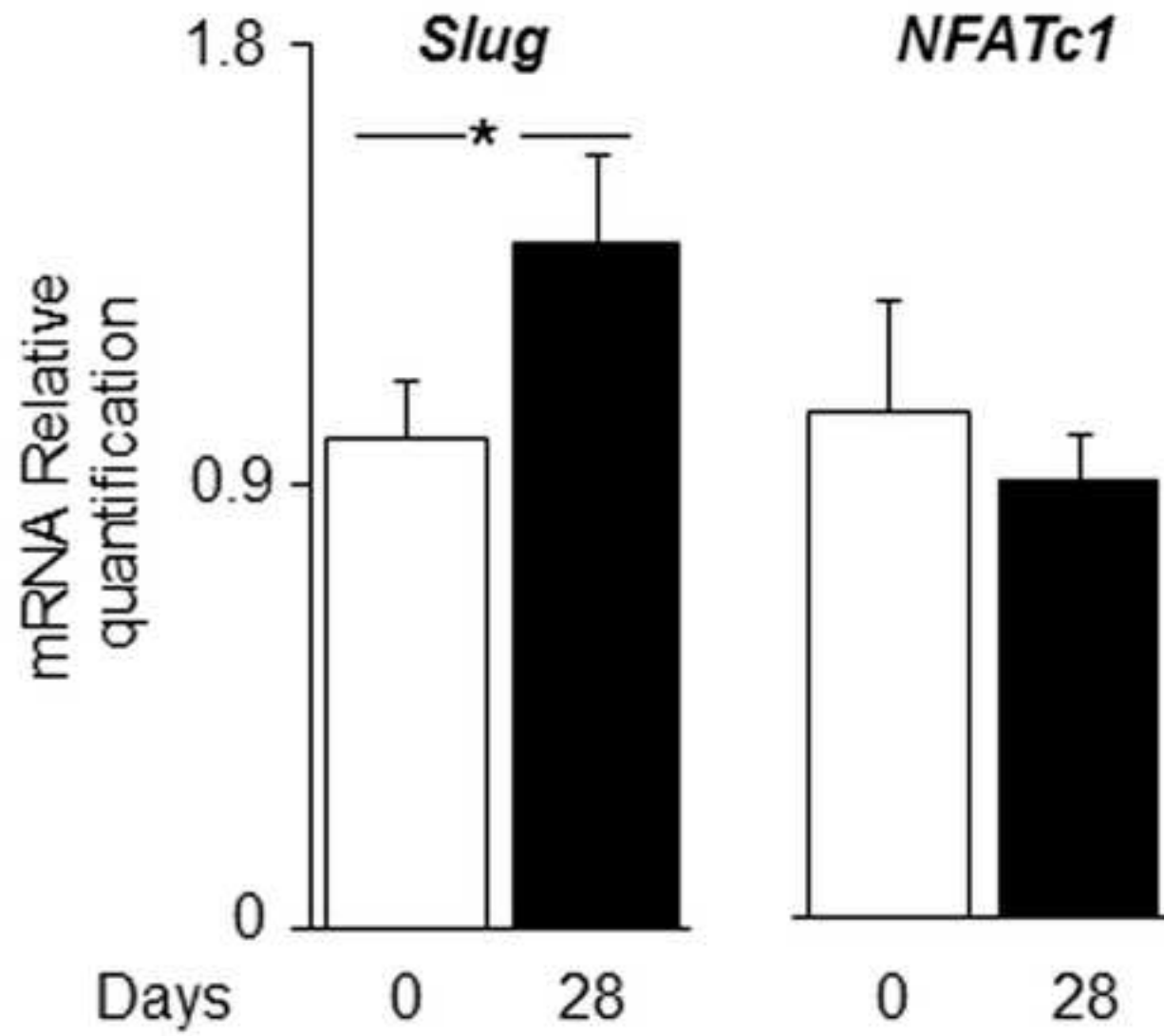


Figure 2 B,C,D

[Click here to download high resolution image](#)

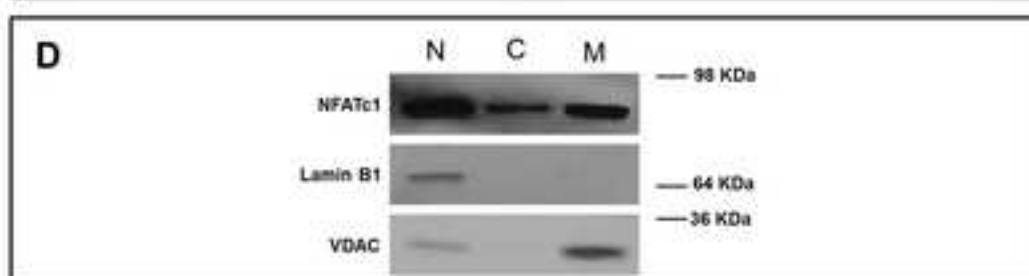
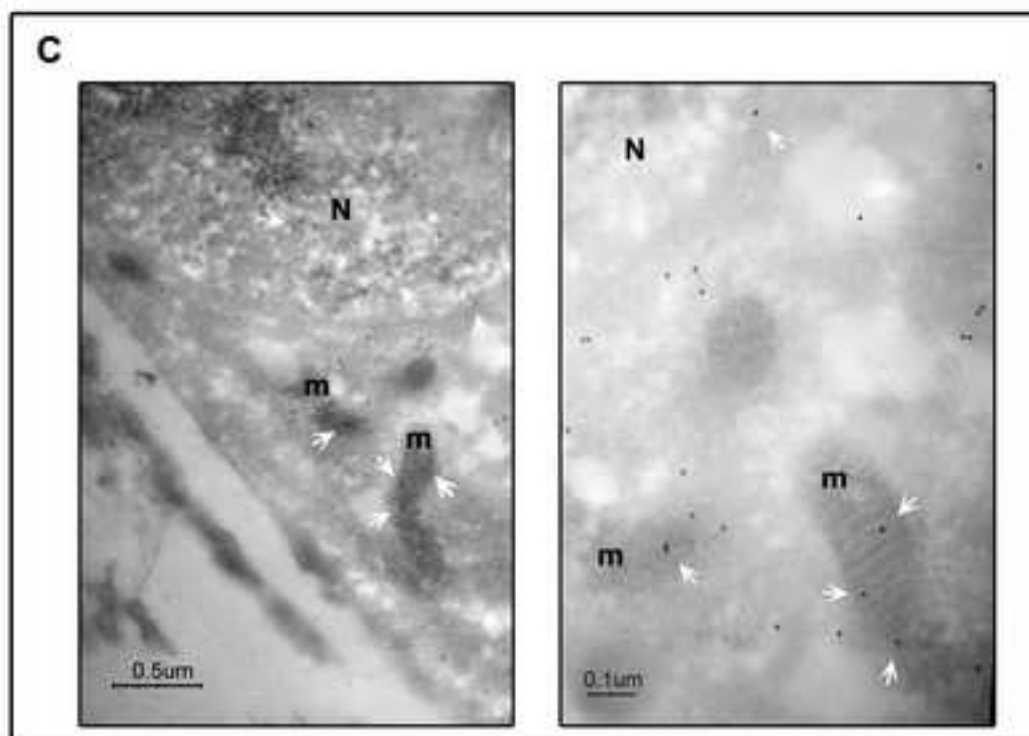
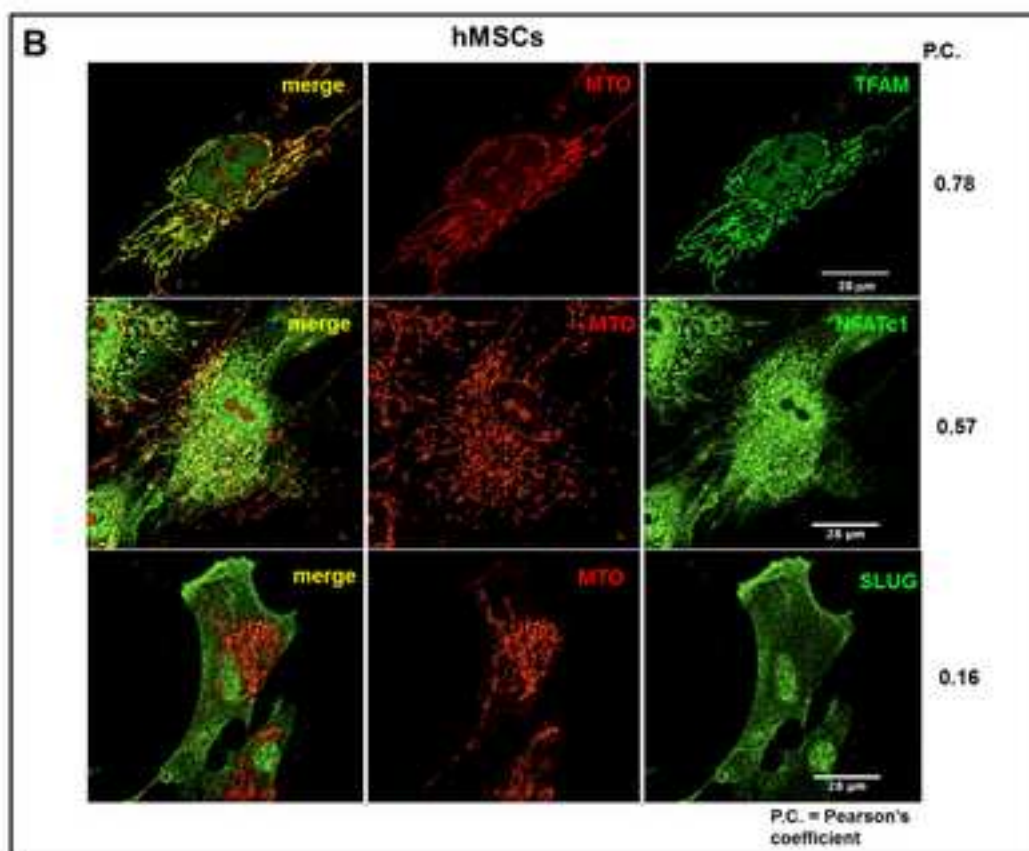


Figure 3
[Click here to download high resolution image](#)

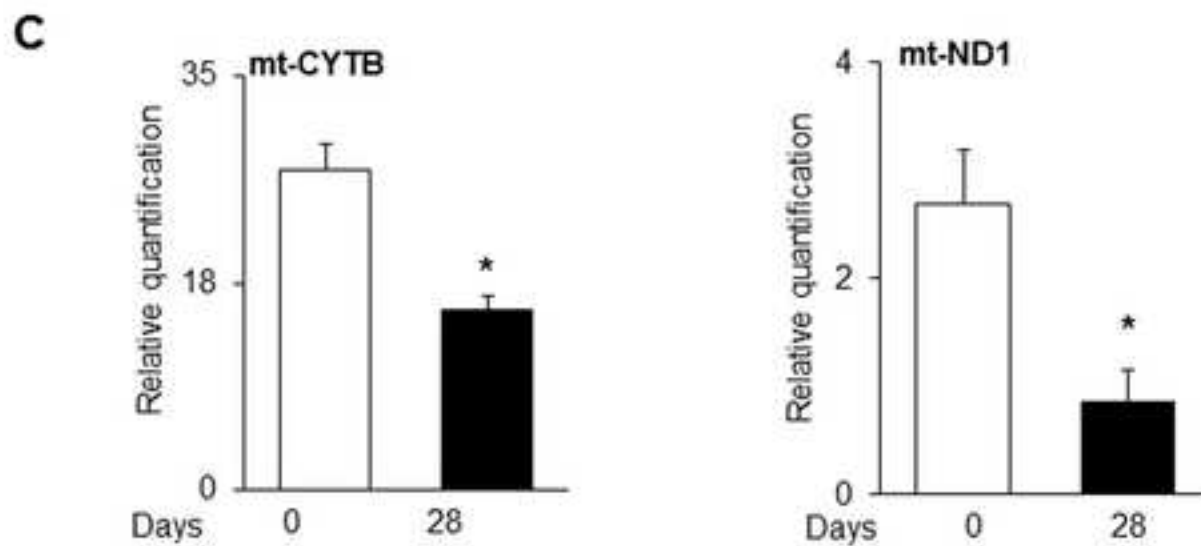
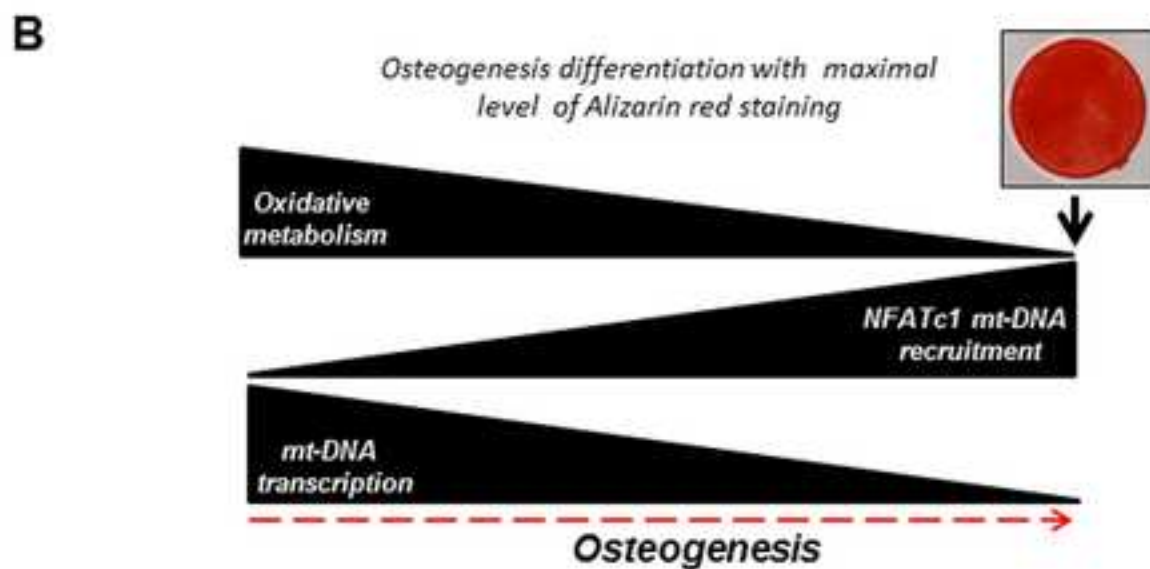
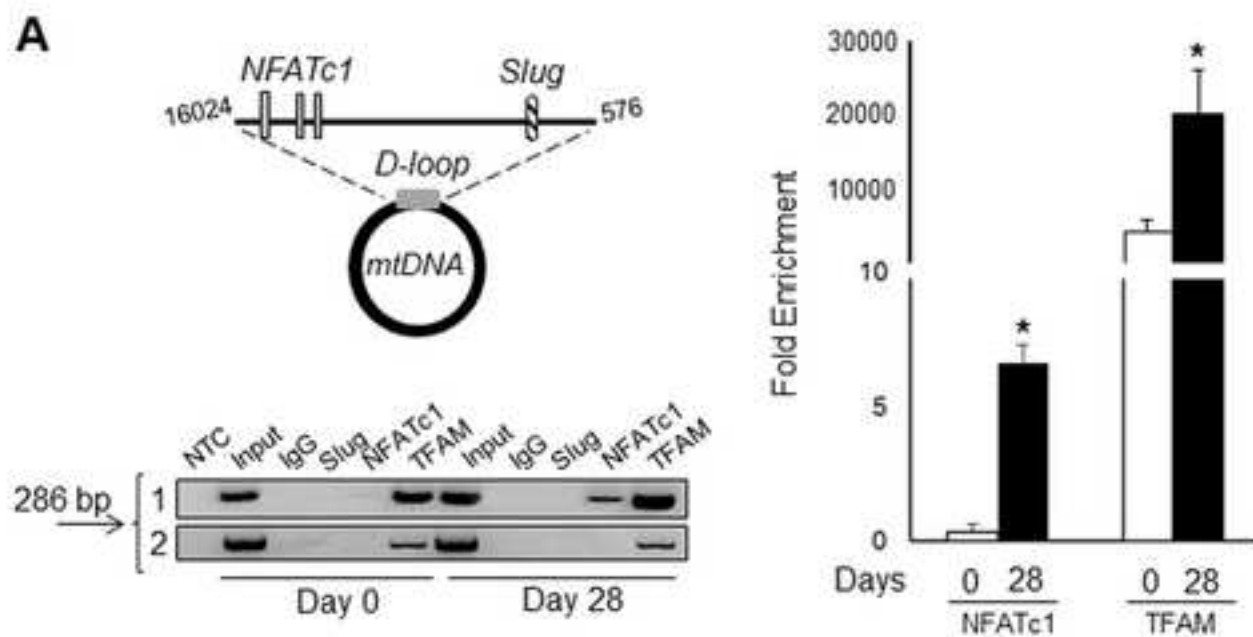


Table 1

[Click here to download high resolution image](#)

Table 1

Prediction of mitochondrial localization of the known NFATc1 isoforms and Slug by the informatical tools MitoProt and target.

Target	TargetP	Mitoprot	
	Predicted subcellular localization	Probability of export	Cleavage sequence
NFATc1 A-alpha	Mitochondria	0.1448	MPSTSFPVPSKFPLGPAAAVFGRGETLGPAPRA
NFATc1 A-alpha'	-	0.0599	NA
NFATc1 B-alpha	Mitochondria	0.1444	MPSTSFPVPSKFPLGPAAAVFGRGETLGPAPRA
NFATc1 B-beta	-	0.0052	NA
NFATc1 C-alpha	Mitochondria	0.1343	MPSTSFPVPSKFPLGPAAAVFGRGETLGPAPRA
NFATc1 C-beta	-	0.0054	NA
NFATc1 IA-deltaIX	Mitochondria	0.1433	MPSTSFPVPSKFPLGPAAAVFGRGETLGPAPRA
NFATc1 IB-deltaIX	-	0.0053	NA
SNAI2	-	0.5571	NA

Supplementary Files

[Click here to download Supplementary Files: Fig. S1 new version.tif](#)